Current Research in Food Science 5 (2022) 1110–1117

Contents lists available at ScienceDirect

Current Research in Food Science

journal homepage: www.sciencedirect.com/journal/current-research-in-food-science

Fabrication of zein-modified starch nanoparticle complexes via microfluidic chip and encapsulation of nisin

Xuanbo Liu, Luis Alberto Ibarra-Sánchez, Michael J. Miller, Youngsoo Lee *

Department of Food Science and Human Nutrition, the University of Illinois at Urbana-Champaign, 382B, Agricultural Engineering and Sciences Building, 1304 W. Pennsylvania Ave., Urbana, IL 61801, USA

ARTICLE INFO

Handling editor: Maria Corradini

Keywords:
Zein nanoparticle
OSA-Modified starch
Microfluidic chip
Stability
Encapsulation
Nisin

ABSTRACT

A microfluidic chip is a micro-reactor that precisely manipulates and controls fluids. Zein is a group of prolamines extracted from corn that can form self-assembled nanoparticles in water or a low concentration of ethanol in a microfluidic chip. However, the zein nanoparticles have stability issues, especially in a neutral pH environment due to the proximity of the isoelectric point. This study was designed 1) to evaluate the effect of octenyl succinic anhydride (OSA) modified starch on the stability of zein nanoparticles formed using a microfluidic chip and 2) to apply the zein-OSA starch for encapsulation of nisin and evaluate its anti-microbial activity in a model food matrix. A T-junction configuration of the microfluidic chip was used to fabricate the zein nanoparticles using 1% or 2% zein solution and 0–10% (w/w) of OSA starch solution. The stability of the nanoparticles in various ionic strength environments was assessed. Encapsulation efficiency and anti-microbial activity of nisin in the zein nanoparticles against *Listeria monocytogenes* in a fresh cheese were measured. As the concentration of OSA starch increased from 0 to 10%, effective diameter increased from 117.8 ± 14.5 to 198.7 ± 13.9 nm without affecting polydispersity indexes and zeta-potential changed toward that of the modified starch indicating the zein surface coverage by the OSA starch. The zein-OSA starch nanoparticle complexes were more stable at various sodium chloride concentrations than the zein nanoparticles without OSA starch. The encapsulation efficiency of nisin was positively correlated with the OSA starch concentration. The anti-microbial activity of nisin in the fresh cheese also increased until 3-days of storage as the concentration of the OSA starch increased, which presented both a potential and challenge toward applications.

1. Introduction

Microfluidic chips are novel micro-reactors that are used to control the ultra-small volume of fluids within the channel dimensions of tens of micrometers. Researchers have been able to expand the application of microfluidic chips in many fields, including drug discovery, biomedical imaging, and biomolecule synthesis (Teh et al., 2008). The diversified application of microfluidics is attributed to their superior ability to precisely control a small segment of liquid, which thereby could be used as reaction confinements (Mark et al., 2010). In terms of food-related applications, the microfluidic chip can be used as the tool for emulsion (Comunian et al., 2018; Priest et al., 2011; Ravanfar et al., 2018; Zhao-Miao et al., 2018), micro-detections (Guo et al., 2015; Kant et al., 2018; Kim et al., 2015), and micro-reactors (Marze et al., 2014; Nguyen, Marquis, Anton and Marze, 2019a, 2019b). There are many advantages for the microfluidic chip: small reagent volumes, selectivity, green credentials, rapid reactions, and small footprints (Elvira et al., 2013). However, very few food-grade materials have been successfully adapted in a microfluidic chip and more studies are needed to explore the applications that require food-grade materials.

Zein is the prolamine protein in corn. More than 50% of its amino acids are hydrophobic, including leucine, proline, and alanine. According to the amino acid sequence and solubility in water, zein can be classified into four distinct types: α-zein, β-zein, γ-zein and δ-zein (Zhang et al., 2011) and among those types, α- is constituted around 70% in total (Lawton, 2002). Zein is widely used in food and pharmaceutical industries because it is generally recognized as safe (GRAS), biodegradable, and biocompatible. Zein can form self-assembled particles by anti-solvent precipitation in the solution at a low ethanol concentration (Lawton, 2002; Patel and Velikov, 2014). However, zein nanoparticles are not stable in the wide range of pH, especially having issues at the isoelectric point at around 6.8. Polysaccharides can be attached to the

* Corresponding author.
E-mail address: leeys@illinois.edu (Y. Lee).

https://doi.org/10.1016/j.crfs.2022.07.005
Received 30 November 2021; Received in revised form 16 June 2022; Accepted 4 July 2022
Available online 12 July 2022

surface of zein nanoparticles to increase stability. The nanoparticles with protein-polysaccharide complex have gained attention in the food, personal care, and pharmaceutical industries because they are easy to prepare, biodegradable, and biocompatible (Chang et al., 2017). Protein-polysaccharide complex has been reported to encapsulate bioactive compounds and increase the encapsulation efficiency and stability of the core materials (Dai et al., 2018). Octenyl-succinic-anhydride (OSA) modified starch has been used in the food industry for more than 40 years (Hui, Qi-he, Ming-liang, Qiong, & Guo-qing, 2009) and is a candidate to form zein nanoparticle complexes. The OSA modified starch is an amphiphilic molecule obtained from the esterification reaction between starch hydroxyl groups and octenyl succinic anhydride and can be used as an emulsion stabilizer and encapsulating agent (Sweedman et al., 2013). OSA-modified starch is negatively charged in the range of pH from 3 to 8 because the branch chain of OSA-modified starch has negative charges in the wide range of pH.

Nisin is a 34-amino acid antimicrobial peptide produced by *Lactococcus lactis* ssp. *Lactis* (Ibarra-Sánchez et al., 2020), and nisin has been considered as generally recognized as safe (GRAS) in the food system by the US Food and Drug Administration (FDA) (21CFR184.1538) (Özel et al., 2018). In the food industry, nisin can be used as the antibacterial agent against Gram-positive pathogens, such as *Listeria monocytogenes* and *Staphylococcus aureus* (Shin et al., 2016). However, nisin has some limitations, such as instability at high temperatures, reduced activity in low acidity and high fat-containing foods, undesirable interactions with other food components, and low water solubility (de Arauz et al., 2009; Ibarra-Sánchez et al., 2020). These limitations can be overcome by encapsulating nisin into nanocarriers, including nanoemulsion, nanoparticles, nanoliposomes, and nano-fibers (Bahrami et al., 2019). In this study, the zein-OSA modified starch nanoparticles were fabricated using the microfluidic chip, and nisin was encapsulated into the zein-OSA modified starch complex. The objectives of this study were 1) to evaluate the effect of OSA modified starch on the properties of zein nanoparticles formed using a microfluidic device and 2) to evaluate the encapsulation efficiency and antilisterial activity of nisin encapsulated in zein-OSA starch nanopartilces using Queso Fresco as a model food matrix.

2. Materials and methods

2.1. Materials

Zein (purified) was purchased from Sigma–Aldrich (St. Louis, MO). Ethanol (200 proof) was purchased from Decon Labs (King of Prussia, PA). And OSA-modified starch was obtained from Ingredion company (Ingredion, Westchester, IL). Nisin (Nisaplin, Danisco, New Century, KS) was extracted with 70% ethanol at pH = 3.0 overnight to prepare the stock solution.

2.2. Sample preparation

The dispersed phase was 1% or 2% zein dissolved in 70% (w/v) ethanol by stirring at 200 rpm overnight in a closed container and then centrifuged at 4000 rpm for 10 min to remove undissolved materials. The continuous phase was a OSA-modified starch solution at various concentrations: 0%, 1%, 2.5%, 5%, 7.5%, and 10% (w/w). The starch was dissolved into the deionized (DI) water by stirring at 200 rpm overnight. pH was adjusted to 3 for both phases. The sample used in this study are listed in the Table 1. The 1% or 2% zein solution was loaded into a 10 ml syringe (Hamilton Robotics, Reno, NV) and the flow rate was set at 10 ml/h which was controlled by a syringe pump (Harvard Apparatus, Holliston, MA). The different concentrations of the modified starch solutions were loaded into the 10 ml syringe (Hamilton Robotics, Reno, NV) and the flow rate was set at 30 ml/h which were controlled by a syringe pump (Harvard Apparatus, Holliston, MA). The T junction, 100 μm microfluidic chip was used to collect samples and each sample was created with triplicates. The microfluidic chip was purchased from Dolomite (Dolomite Ltd., Royston, UK). The nanoparticle dispersions were collected in 20 mL glass vials (Thermo Fisher Scientific, Inc., Waltham, MA) for analyses.

Table 1
The sample codes of zein-modified starch nanoparticles formation via microfluidic chip.

The sample code	OSA-Modified Starch Concentration% (w/w)	Zein Concentration% (w/w)
MS0-Zein1	0	1
MS1-Zein1	1	
MS2.5-Zein1	2.5	
MS5-Zein1	5	
MS7.5-Zein1	7.5	
MS10-Zein1	10	
MS0-Zein2	0	2
MS1-Zein2	1	
MS2.5-Zein2	2.5	
MS5-Zein2	5	
MS7.5-Zein2	7.5	
MS10-Zein2	10	

2.3. Particle size and polydispersity index determination

All the samples were diluted at 1:40 using the DI water and the effective diameter was measured by the Dynamic Light Scattering (DLS) particle size analyzer (Brookhaven Instruments, Holtsville, NY). The effective diameters were reported as the surface average diameter (D3,2) and the equation was expressed as follow:

$$D3,2 = \frac{\Sigma nidi^3}{\Sigma nidi^2} \quad (1)$$

where ni is the number of particles with diameter di. The three replicated readings were collected for each sample. The polydispersity index (PDI) was also obtained by the DLS and three replicated readings were averaged.

2.4. Zeta-potential measurements

The zeta-potential of the freshly prepared samples were measured by the zeta-potential analyzer (Brookhaven Instruments, Holtsville, NY) at the various pH values from 3 to 8. The suspensions were diluted by 80 times to minimize the electrokinetic potential not a contribution from inter-colloidal interaction.

2.5. Interactions related to the formation of the particle

The contributions of hydrogen bonding, hydrophobic interaction, and disulfide bonding for particle formation were evaluated by the urea, sodium dodecyl sulfate (SDS), and dithiothreitol (DTT), respectively according to the previously published method (Akbari and Wu, 2016). The zein-nanoparticle solutions with different concentrations of the OSA-modified starch were mixed with the agents at various concentrations to assess the driving force for the complex formation. For the urea, the concentration was varied from 1M to 7 M, from 0.25% to 1% (w/w) for SDS, and from 10 mM to 60 mM for DTT. After 6 h, the turbidity of the solutions was measured by the UV–visible spectrophotometer (Genesys5, Thermo Scientific Co., Waltham, MA) at 600 nm wavelengths. T_0 was the initial turbidity of the solutions and T was the turbidity of the solutions after adding the dissociation agents. The ratio of the T/T_0 was used to indicate the dissociation of the particles.

2.6. The stability of the particles in the salt solution

The stability of the zein-nanoparticles was measured by adding the particles to various concentrations of sodium chloride (NaCl) solutions and the sedimentation was observed (H. Chen and Zhong, 2015). The same volume of the NaCl solution was combined with the freshly prepared zein-nanoparticles solution with different concentrations of the modified starch (0%, 1%, 2.5%, 5%, 7.5%, and 10%). The final NaCl concentrations in the mixture were 0 mM, 25 mM, 50 mM, and 125 mM.

2.7. Circular dichroism (CD) spectroscopy

The CD spectra were collected using JASCO J-715 spectropolarimeter (Jasco Inc., Easton, MD) and the method in a previous publication was used with some modifications (Feng and Lee, 2017). The 100 times diluted samples were placed in an 1 cm path length quartz cell, and the wavelength ranged from 200 to 250 nm at 25 °C with the scanning speed of 50 nm/min. The ratio of the α-helix, β-sheet, and the random coil was calculated by the BeStSel software (Micsonai et al., 2015).

2.8. The encapsulation efficiency of nisin

2.8.1. Encapsulation of nisin

Nisin was dissolved to reach 0.5 mg/ml in 1% or 2% zein in 70% (w/v) ethanol solution as the dispersed phase by stirring at 200 rpm overnight and then centrifuged at 4000 rpm for 10 min to remove unsolvable materials. The continuous phase was prepared by dissolving OSA-modified starch into the DI water to reach various concentrations (0%, 5%, and 10% (w/w)) by stirring the solution at 200 rpm overnight to ensure complete hydration of the modified starch. pH was adjusted to 3 for both phases. The 1% or 2% zein solution with nisin was loaded into the 10 ml syringe (Hamilton Robotics, Reno, NV) and the flow rate was 10 ml/h which was controlled by a syringe pump (Harvard Apparatus, Holliston, MA). The modified starch solutions were loaded into the 10 ml syringe (Hamilton Robotics, Reno, NV) and the flow rate was 30 ml/h which were controlled by a syringe pump (Harvard Apparatus, Holliston, MA). The T junction 100 μm microfluidic chip was used to collect samples with three batch replicates. The nanoparticle dispersions were collected in 20 mL glass vials (Thermo Fisher Scientific, Inc., Waltham, MA) for analyses.

2.8.2. Nisin encapsulation efficiency

To quantify nisin in the nanocapsules suspensions, 300 μL of nanocapsule suspension was mixed with 700 μL of 100% ethanol to disrupt nanocapsules and release nisin for total nisin, or mixed with 700 μL of deionized water to maintain nanocapsules integrity to measure free nisin in the supernatant. Samples were passed sequentially through 0.45, 0.22, and 0.1 μm filters (PES Syringe Filter, Sartorius) to separate polymer fractions or microcapsules from the solution before injecting into an HPLC for nisin quantification. The encapsulation efficiency was calculated as follows:

$$Encapsulationefficiency(\%) = \frac{(totalamountofnisin - freenisininthe\ supernant)}{total\ amount\ of\ nisin} \times 100$$

2.8.3. Nisin quantification with HPLC

Nisin was quantified utilizing HPLC as previously described with minor modifications (Feng et al., 2019). Briefly, a Waters 2695 Alliance HPLC system (Waters, Milford, MA) equipped with a Hewlett-Packard series 1050 photodiode array detector (Hewlett-Packard, Palo Alto, CA) was used. The analytical column was a reversed-phase Hypersil GOLD C18 (175 A, 250 × 4.6 mm, 5 μm) (Thermo Scientific, San Diego, CA). Solvent A was 0.1% (v/v) trifluoroacetic acid (TFA) in ultra-pure water, and solvent B was 90% (v/v) HPLC-grade acetonitrile (Thermo Fisher Scientific) containing 0.1% TFA (v/v) in ultra-pure water. The column temperature was maintained at 40 °C, sample injection volume was 20 μL, and samples were measured at UV absorption of 214 nm. A linear gradient from 31% B to 43% B over 16 min was run at a flow rate of 1.0 mL/min. The standard curve was plotted using 10, 50, 100, 200, and 300 μg/mL nisin (Nisaplin®, 2.5% nisin w/w), and the amount of nisin was calculated from the area of the peak at 214 nm. HPLC analysis was performed in duplicate for each sample.

2.9. The antimicrobial test

2.9.1. Microorganisms and culture conditions

Listeria monocytogenes strains (Agricultural Research Service Culture Collection Northern Regional Research Laboratory strains B-33104, B33419, B-33420, B-33424, and B-33513) were recovered from frozen glycerol stock (−80 °C) and grown in brain heart infusion (BHI; Difco, Becton Dickinson and Co., Sparks, MD) broth, at 37 °C for 24 h with 250-rpm agitation to obtain cell concentrations of ~9 Log CFU/mL. *L. monocytogenes* cocktails were prepared by combining equal volumes of stationary phase cultures of the five different foodborne outbreak-associated strains. The serial dilutions of the *L. monocytogenes* cocktail were further prepared in PBS (KCl 200 mg/L; KH_2PO_4, 200 mg/L; NaCl, 8 g/L; Na_2HPO_4, 1.15 g/L, pH 7.2) to obtain the desired cell concentrations. *Listeria* enumeration was carried out on PALCAM Listeria-Selective agar (EMDMillipore) supplemented with 20 mg/mL ceftazidime (Tokyo Chemical Industry Co. Ltd.) and incubated for 48 h at 37 °C.

2.9.2. Antilisterial properties in Queso Fresco

The antimicrobial activity of free and encapsulated nisin was evaluated by their addition to Queso Fresco (QF) as previously described with minor modifications (Van Tassell et al., 2015). Aliquots of microcapsule suspensions containing 37.5 μg nisin were vacuum concentrated in a Vacufuge Concentrator 5301 (Eppendorf North America, Westbury, NY, USA) for 45 min at room temperature. Batches of QF were prepared with Nisaplin® and concentrated microcapsules suspension to an equivalent amount of 37.5 μg of nisin/mL of milk added into the milk before renneting. This corresponded to approximately 250 μg of nisin/g of cheese, the maximum permissible concentration in the United States. Sample cheeses were inoculated with a five-strain *L. monocytogenes* cocktail directly into the curd before pressing, for a final concentration of approximately 3.5 Log CFU/g. All cheeses were stored at 4 °C for up to 14 days until sampled for *Listeria* enumeration. Cheeses were individually homogenized and serially diluted in PBS and spread plated on PALCAM Listeria-Selective agar supplemented with 20 μg/mL ceftazidime to enumerate *L. monocytogenes*. Plates were incubated at 37 °C for 48 h.

2.10. Statistical analysis

All the experimental results were conducted in triplicate. The results were expressed as mean ± standard deviation (n = 3). The significant differences of the results among the different treatments were conducted by ANOVA ($P < 0.5$), and the averages were compared using Tukey's test.

3. Results and discussion

3.1. Particle size and polydispersity index (PDI)

The particle size and polydispersity index (PDI) of the 1% and 2% zein nanoparticles with the various concentration of the OSA-modified starch (0%, 1%, 2.5%, 5%, 7.5%, and 10%) are shown in Fig. 1. As the concentration of OSA-modified starch increased, the particle size of the zein-nanoparticles increased. The particle size of the zein-

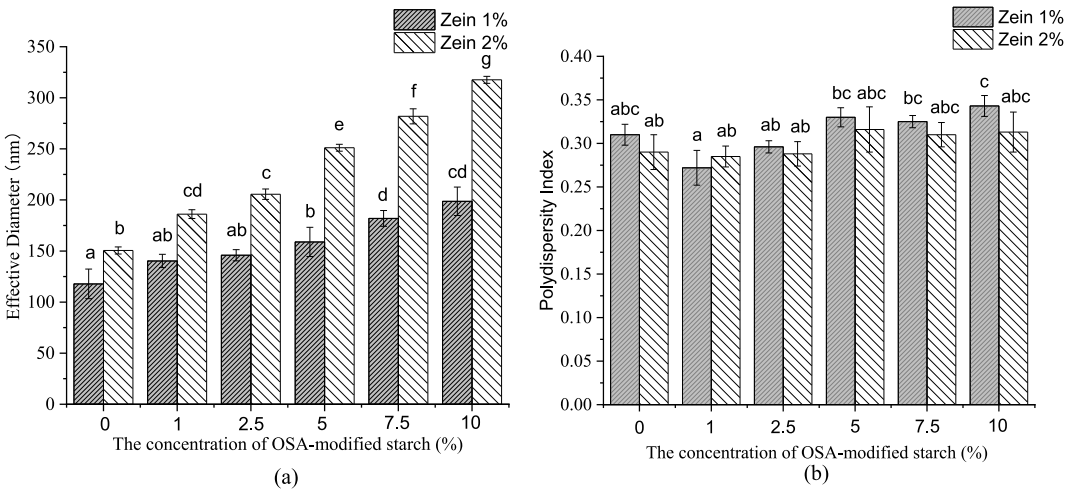

Fig. 1. The effective diameter (a) and PDI (b) of the 1%, and 2% zein nanoparticles with various concentrations of modified starch.

nanoparticle without the modified starch was around 117.8 nm, which is in good agreement with the previously reported results (H. Chen and Zhong, 2015; Gonçalves da Rosa et al., 2020). As the concentration of OSA-modified starch increased from 1% to 10%, the effective diameter increased from 117.8 ± 14.5 to 198.7 ± 13.9 nm with the 1% of zein solution and from 150.53 ± 3.48 to 317.6 ± 3.4 nm with the 2% of zein solutions. The effective diameter increased as the concentration of OSA-modified starch increased because the addition of modified starch attached to the surface of zein nanoparticles to enlarge the particle size. Although there were statistical differences in the PDI in the zein-nanoparticle with various concentrations of the modified starch, there was no clear trend. The PDI describes the degree of "non-uniformity" of the distribution, which indicated the addition of modified starch did not change the uniformity of the zein nanoparticles fabricated in the microfluidic chip.

3.2. Zeta-potential

The zeta-potential of the 1% and 2% zein nanoparticles with the various concentrations of OSA-modified starch are shown in Fig. 2. For the zein nanoparticles without OSA-modified starch, as the pH increased from 3 to 8, the zeta-potential changed from the positive to the negative, and the isoelectric point (pI) of the zein was around 6.4, which is in good agreement with the published results (H. Chen and Zhong, 2015; Hu and McClements, 2015; Li et al., 2019). The zeta-potential of OSA-modified starch is negative in the range of pH from 3 to 8 because the branch chain of OSA-modified starch has negative charges in the wide range of pH (Lin et al., 2018). The concentration of modified starch can be categorized in three levels: low concentration (1% and 2.5%), medium concentration (5% and 7.5%), and high concentration (10%). For the 1% zein solution with the low concentration of modified starch, as the pH increased, the zeta-potential changed from positive to negative, and the pI was around 4 which is lower than the zein only nanoparticles. With the medium and high concentration of modified starch, the zeta-potential was negative in the entire pH range from 3 to 8. For the 2% zein solution with the low and medium concentration of modified starch, as the pH increased, the zeta-potential changed from positive to negative, and the pI was around 3.3. With the high concentration of modified starch, the zeta-potential was negative in the entire pH range from 3 to 8. At the low modified starch concentration, the modified starch only partially covered the surface of the zein nanoparticles. As the starch concentration increased, the modified starch increased the coverage of the zein surface of the zein nanoparticles. Eventually, the zein nanoparticle surface was fully covered by the starch. The results also suggest that the electrostatic interaction was one of the main driving forces to form the zein OSA-modified starch nanoparticles (S. Chen et al., 2020).

3.3. Interactions related to the formation of the particle

Different interactions such as hydrogen bonding, electrostatic interaction, disulfide bonding, and hydrophobic interactions could affect the zein OSA-modified starch nanoparticles formation. To understand the driving force between zein and OSA-modified starch, different dissociation agents were used. The SDS disrupted the hydrophobic interactions among the zein-modified starch, and the urea and

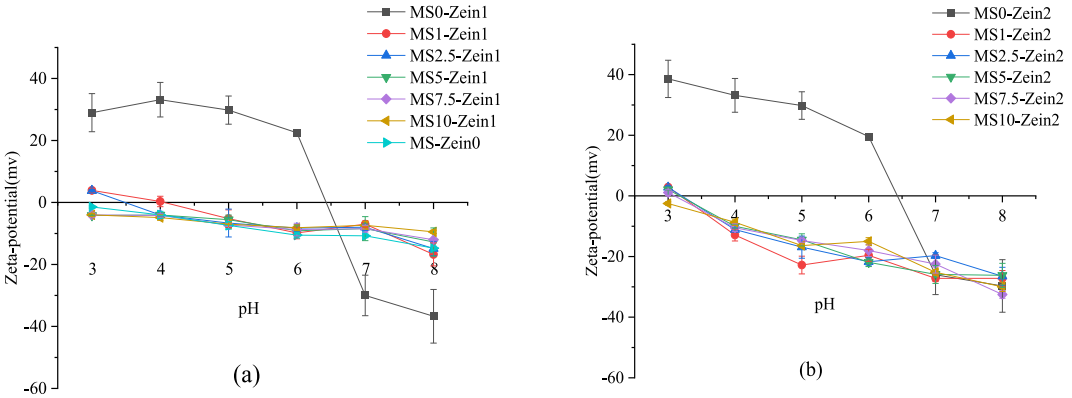

Fig. 2. The zeta-potential of zein nanoparticle with different concentrations of modified starch.(a) 1% zein nanoparticles; (b) 2% zein nanoparticles.

DTT tested the hydrogen bonding and disulfide bonding, respectively. The ratio of the T/T_0 was used to indicate the dissociation particles. As SDS and urea were added, the zein OSA-modified starch dissociated and the turbidity of the suspension decreased due to the disrupted interactions. As shown in Fig. 3 with the concentration of the SDS and urea increased, the T/T_0 decreased. However, as the concentration of the DTT increased, the T/T_0 did not change. The results indicated that the hydrophobic interactions and hydrogen bonding were the main driving force to form the zein-modified starch nanoparticles via microfluidic chip (Akbari and Wu, 2016).

3.4. Stability of the particles in salt solution

Fig. 4 shows the visual observation of the zein-modified starch nanoparticles in a series of NaCl solutions. As the concentration of the NaCl increased, the stability of the nanoparticles decreased and aggregated more. For the same concentration of NaCl, as the concentration of the modified starch increased, the stability of the zein nanoparticles increased and less aggregates were observed. The modified starch could increase the stability of the zein nanoparticles within 0–125 mM of NaCl solution. The increased stability in elevated NaCl concentration provides expands application of the nanoparticles as many food products such as fresh cheeses and salad dressings.

3.5. Circular dichroism (CD) spectroscopy

The circular dichroism spectroscopy of the 1% and 2% zein nanoparticles with different concentrations of the modified starch (0%, 5%, and 10%) are shown in Table 2 and Fig. 5. In the CD spectra, individual zein nanoparticles and zein OSA-modified starch exhibited two troughs at 210 nm and 225 nm. For the untreated zein nanoparticles, the fractions of α-helix, β-sheet, and random coil were around: 14%, 43%, and

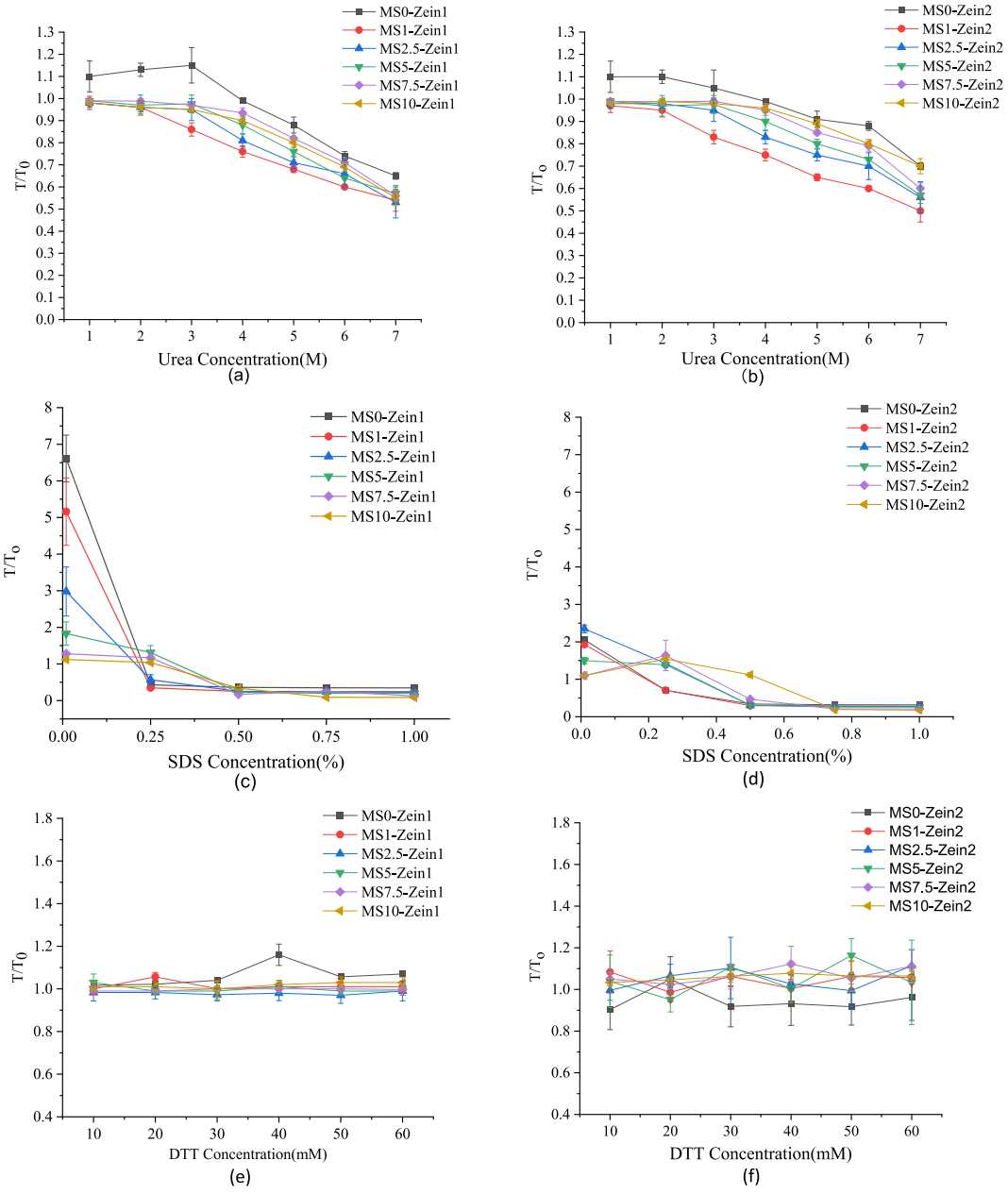

Fig. 3. The effect of the Urea, SDS, and DDT on change of the turbidity of the zein-modified starch nanoparticle. (a), (c), (e) 1% zein nanoparticles; (b), (d), (f) 2% zein nanoparticles.

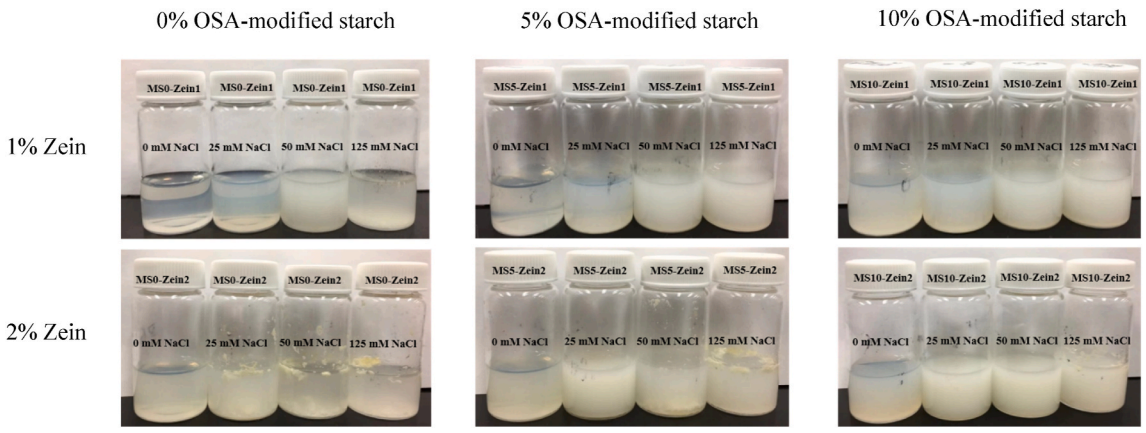

Fig. 4. The pictures of the zein-modified starch nanoparticles in a series of NaCl concentrations.

Table 2
The CD Spectroscopy results of the zein-nanoparticle with 0, 5, and 10% modified starch.

The sample	α-helix (%)	β-sheet (%)	Random coil (%)
MS0-Zein1	14.8 ± 1.35[a]	43 ± 2.69[a]	42.2 ± 2.35[a]
MS5-Zein1	12.8 ± 1.07[a]	44.2 ± 1.52[a]	43 ± 1.65[a]
MS10-Zein1	11 ± 0.96[a]	43.5 ± 0.78[a]	45.5 ± 2.17[a]
MS0-Zein2	14 ± 0.86 [a]	41.2 ± 1.45[a]	44.8 ± 1.07[a]
MS5-Zein2	13.6 ± 0.93 [a]	47.9 ± 2.96[b]	38.5 ± 2.78[b]
MS10-Zein2	11.9 ± 0.65 [a]	42.6 ± 1.02[a]	45.5 ± 1.98[a]

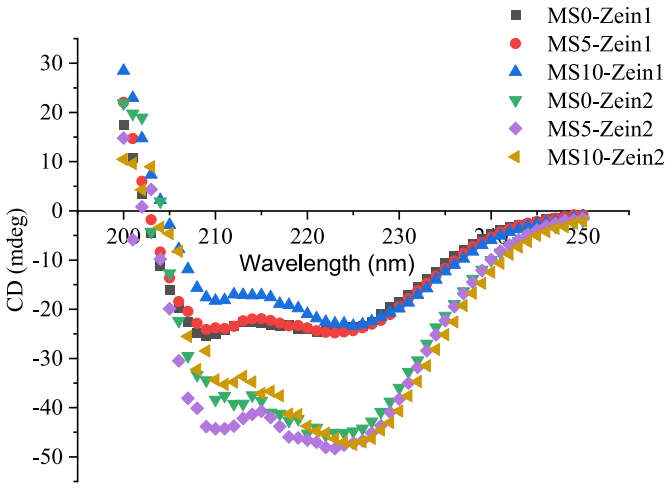

Fig. 5. The CD Spectra of the zein-nanoparticle with 0, 5, and 10% the modified starch.

43% which is in good agreement with the literature (Feng and Lee, 2017). Compared with the zein nanoparticles, there was no significant difference in the ratio of α-helix, β-sheet, and random coil among the various concentration of the zein OSA-modified starch complex. The results showed that the modified starch did not change the secondary structure of zein in the nanoparticles.

3.6. The encapsulation efficiency of nisin

The encapsulation efficiency of the nisin in the 1% and 2% zein nanoparticles with the various concentration of modified starch (0%, 5%, and 10%) was showed in Fig. 6. As the concentration of the modified starch increased, the encapsulation efficiency of nisin increased. For the 1% zein nanoparticles, the encapsulation efficiency enhanced from 10%

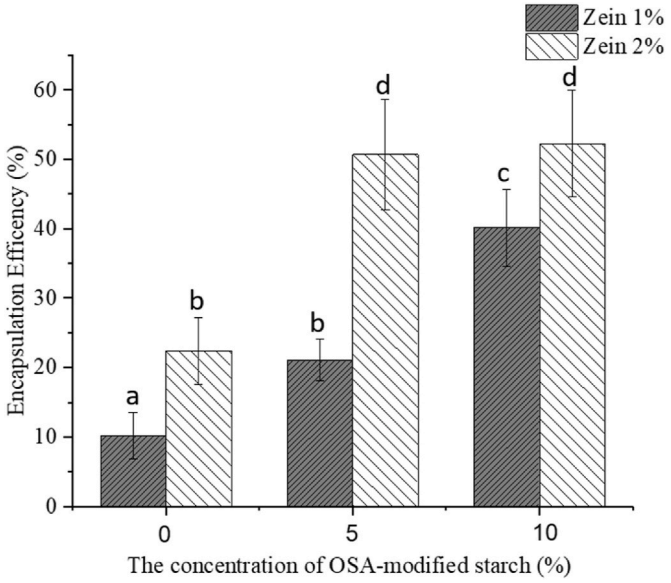

Fig. 6. The encapsulation efficiency of the nisin encapsulated zein nanoparticle with 0, 5, and 10% modified starch.

to 40%, and for the 2% zein nanoparticles, the encapsulation efficiency increased from 23% to 50%. The results are probably due to the increased wall thickness on the zein surface which is indirectly presented with particle size (Fig. 1), zeta potential (Fig. 2), and CD (Table 2) data. When the OSA-modified starch attached to the surface of zein nanoparticles, the particle size increased and the thicker layer of OSA-modified starch provides more space as well as a barrier for nisin to be encapsulated thus encapsulation efficiency increased.

3.7. The antimicrobial test

Nisin is known to inhibit Gram-positive bacteria, such as *L. monocytogenes*, a foodborne pathogen that has been associated with listeriosis outbreaks linked to fresh cheeses (Ibarra-Sánchez et al., 2018). Nisin antimicrobial activity relies on its ability to form pores on Gram-positive bacteria cell wall: nisin inhibits peptidoglycan synthesis by forming a complex with Lipid II, and nisin insertion permeabilizes the cytoplasmic membrane, which allows the efflux of cytoplasmic content and subsequent death of bacteria (Gharsallaoui et al., 2016). The antimicrobial activity of nisin encapsulated in zein-modified starch against *L. monocytogenes* was evaluated in Queso Fresco (Fig. 7). *L. monocytogenes* counts in control cheeses reached approximately 5.5

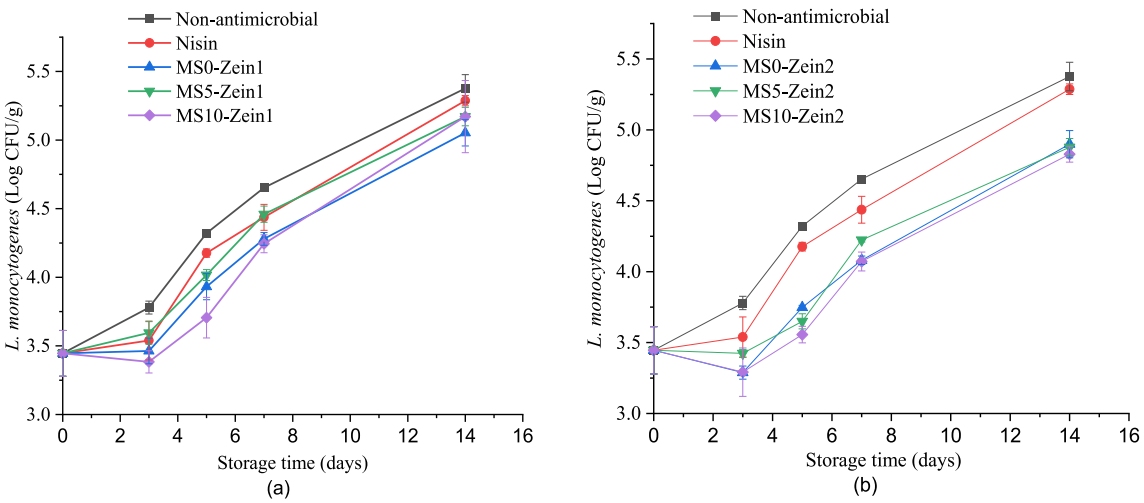

Fig. 7. Antimicrobial activity nisin encapsulated zein nanoparticle with 0, 5, and 10% modified starch. (a) 1% zein nanoparticles; (b) 2% zein nanoparticles.

Log CFU/g by day 14 of storage at 4 °C, an increase of about 2 Log CFU from the initial inoculum. Similar to our previous studies (Feng et al., 2019; Ibarra-Sánchez et al., 2021; Ibarra-Sánchez et al., 2018; Martínez-Ramos et al., 2020), a discreet reduction in the pathogen counts was observed in cheeses added with free nisin compared to control cheeses. The limited antilisterial efficacy of nisin in Queso Fresco is the result of nisin's instability at near-neutral pH, and interactions with milk fat, caseins, and cations (Ibarra-Sánchez et al., 2020). Nisin was encapsulated to overcome the limited anilisterial efficacy of free nisin in fresh cheeses. All cheeses added with nisin encapsulated in zein-modified starch exhibited overall lower pathogen counts during storage. The antilisterial effect of the encapsulated nisin was evident compared to the free nisin until day3. From day 5 until day 14, a difference of approximately 0.5 and 0.8 Log CFU/g relative to control cheeses, was observed in cheeses with nisin in 1% and 2% zein nanoparticles, respectively. However, different concentrations of modified starch (0%, 5%, and 10%) had a negligible impact on enhancing the efficacy of encapsulated nisin to reduce *L. monocytogenes* counts in Queso Fresco samples. Based these observations, it was hypothesized that the location of encapsulated nisin will significantly impact the efficacy of the nisin on *Listeria* in fresh cheese. Although we observed that increasing the concentration of modified starch increased the encapsulation efficiency of nisin in zein nanoparticles (Fig. 6), it is possible that nisin encapsulated on or near the surface (layer of OSA modified starch) was released quickly (e.g. during cheesemaking), and nisin encapsulated into the deeper section of zein nanoparticles were released later to be active against *L. monocytogenes* in Queso Fresco. This hypothesis need further studies to be tested.

4. Conclusions

Zein, a food grade biopolymer, was able form self-assembled nanoparticles using a microfluidic device, which may expand the application of microfluidic devices to the food industry. Specifically, zein OSA-modified starch nanoparticles were prepared by a microfluidic chip with a fixed flow rate at pH 3. As the concentration of the modified starch increased, the particle size and turbidity increased, so the particle size can be controlled by adjusting the formulation. The impact of zein or modified starch concentrations on the PDI was not significant. The main driving forces to form the complex nanoparticles were hydrophobic interaction, electrostatic interaction, and hydrogen bonding. The modified starch did not change the secondary structure of the zein nanoparticles during formation. The incorporation of OSA modified starch enhanced the stability of zein nanoparticles which is a critical properties for applications in foods. The concentration of the modified starch showed a significant effect on the encapsulation efficiency of the nisin but did not show a significant impact on the antimicrobial activity against *L. monocytogenes* tested in Queso Fresco samples. However, the antilisterial effect of the encapsulated nisin was still limited to storage of up to 3 days. So, achieving prolonged antiliterial effect should be the focus of future studies by characterizing the detailed structure of nanocapsules and enhanced release control.

CRediT authorship contribution statement

Xuanbo Liu: The role and contribution of the authors are. **Luis Alberto Ibarra-Sánchez:** design and perform experiments, collect and analyze data, and prepared the manuscript, Formal analysis, Data curation. **Michael J. Miller:** design and perform experiments on fresh cheese, collect and analyze microbial data, and contribute to manuscript preparation, Formal analysis, Data curation. **Youngsoo Lee:** advise researchers and manage fresh cheese experiments and microbial data analysis as well as review the draft manuscript, Writing – original draft, Formal analysis, Data curation.

Declaration of competing interest

The authors declare that they have no known competing financial interests or personal relationships that could have appeared to influence the work reported in this paper.

Acknowledgements

This study has been partially supported by the United State Department of Agriculture, Hatch ILL-330.

References

Akbari, A., Wu, J., 2016. Cruciferin nanoparticles: preparation, characterization and their potential application in delivery of bioactive compounds. Food Hydrocolloids 54, 107–118. https://doi.org/10.1016/j.foodhyd.2015.09.017.

Bahrami, A., Delshadi, R., Jafari, S.M., Williams, L., 2019. Nanoencapsulated nisin: an engineered natural antimicrobial system for the food industry. Trends Food Sci. Technol. 94 (May), 20–31. https://doi.org/10.1016/j.tifs.2019.10.002.

Chang, C., Wang, T., Hu, Q., Luo, Y., 2017. Caseinate-zein-polysaccharide complex nanoparticles as potential oral delivery vehicles for curcumin: effect of polysaccharide type and chemical cross-linking. Food Hydrocolloids 72, 254–262. https://doi.org/10.1016/j.foodhyd.2017.05.039.

Chen, H., Zhong, Q., 2015. A novel method of preparing stable zein nanoparticle dispersions for encapsulation of peppermint oil. Food Hydrocolloids 43. https://doi.org/10.1016/j.foodhyd.2014.07.018, 593e602-602.

Chen, S., Li, Q., McClements, D.J., Han, Y., Dai, L., Mao, L., Gao, Y., 2020. Co-delivery of curcumin and piperine in zein-carrageenan core-shell nanoparticles: formation,

structure, stability and in vitro gastrointestinal digestion. Food Hydrocolloids 99 (August 2019), 105334. https://doi.org/10.1016/j.foodhyd.2019.105334.
Comunian, T.A., Ravanfar, R., Alcaine, S.D., Abbaspourrad, A., 2018. Water-in-oil-in-water emulsion obtained by glass microfluidic device for protection and heat-triggered release of natural pigments. Food Res. Int. 106 (September 2017), 945–951. https://doi.org/10.1016/j.foodres.2018.02.008.
Dai, L., Li, R., Wei, Y., Sun, C., Mao, L., Gao, Y., 2018. Fabrication of zein and rhamnolipid complex nanoparticles to enhance the stability and in vitro release of curcumin. Food Hydrocolloids 77, 617–628. https://doi.org/10.1016/j.foodhyd.2017.11.003.
de Arauz, L.J., Jozala, A.F., Mazzola, P.G., Vessoni Penna, T.C., 2009. Nisin biotechnological production and application: a review. Trends Food Sci. Technol. 20 (3–4), 146–154. https://doi.org/10.1016/j.tifs.2009.01.056.
Elvira, K.S., i Solvas, X.C., Wootton, R.C.R., deMello, A.J., 2013. The past, present and potential for microfluidic reactor technology in chemical synthesis. Nat. Chem. 5 (11), 905–915. https://doi.org/10.1038/nchem.1753.
Feng, Y., Ibarra-Sánchez, L.A., Luu, L., Miller, M.J., Lee, Y., 2019. Co-assembly of nisin and zein in microfluidics for enhanced antilisterial activity in Queso Fresco. LWT (Lebensm.-Wiss. & Technol.) 111 (February), 355–362. https://doi.org/10.1016/j.lwt.2019.05.059.
Feng, Y., Lee, Y., 2017. Microfluidic fabrication of hollow protein microcapsules for rate-controlled release. RSC Adv. 7 (78), 49455–49462. https://doi.org/10.1039/c7ra08645h.
Gharsallaoui, A., Oulahal, N., Joly, C., Degraeve, P., 2016. Nisin as a food preservative: Part 1: physicochemical properties, antimicrobial activity, and main uses. Crit. Rev. Food Sci. Nutr. 56 (8), 1262–1274. https://doi.org/10.1080/10408398.2013.763765.
Gonçalves da Rosa, C., Zapelini de Melo, A.P., Sganzerla, W.G., Machado, M.H., Nunes, M.R., Vinicius de Oliveira Brisola Maciel, M., Manique Barreto, P.L., 2020. Application in situ of zein nanocapsules loaded with Origanum vulgare Linneus and Thymus vulgaris as a preservative in bread. Food Hydrocolloids 99 (August 2019), 105339. https://doi.org/10.1016/j.foodhyd.2019.105339.
Guo, L., Feng, J., Fang, Z., Xu, J., Lu, X., 2015. Application of microfluidic "lab-on-a-chip" for the detection of mycotoxins in foods. Trends Food Sci. Technol. 46 (2), 252–263. https://doi.org/10.1016/j.tifs.2015.09.005.
Hu, K., McClements, D.J., 2015. Fabrication of biopolymer nanoparticles by antisolvent precipitation and electrostatic deposition: zein-alginate core/shell nanoparticles. Food Hydrocolloids 44, 101–108. https://doi.org/10.1016/j.foodhyd.2014.09.015.
Hui, R., Qi-he, C., Ming-liang, F., Qiong, X., Guo-qing, H., 2009. Preparation and properties of octenyl succinic anhydride modified potato starch. Food Chem. 114 (1), 81–86. https://doi.org/10.1016/j.foodchem.2008.09.019.
Ibarra-Sánchez, L.A., El-Haddad, N., Mahmoud, D., Miller, M.J., Karam, L., 2020. Invited review: advances in nisin use for preservation of dairy products. J. Dairy Sci. 103 (3), 2041–2052. https://doi.org/10.3168/jds.2019-17498.
Ibarra-Sánchez, L.A., Kong, W., Lu, T., Miller, M.J., 2021. Efficacy of nisin derivatives with improved biochemical characteristics, alone and in combination with endolysin PlyP100 to control Listeria monocytogenes in laboratory-scale Queso Fresco. Food Microbiol. 94 (July 2020) https://doi.org/10.1016/j.fm.2020.103668.
Ibarra-Sánchez, L.A., Van Tassell, M.L., Miller, M.J., 2018. Antimicrobial behavior of phage endolysin PlyP100 and its synergy with nisin to control Listeria monocytogenes in Queso Fresco. Food Microbiol. 72, 128–134. https://doi.org/10.1016/j.fm.2017.11.013.
Kant, K., Shahbazi, M.A., Dave, V.P., Ngo, T.A., Chidambara, V.A., Than, L.Q., et al., 2018. Microfluidic devices for sample preparation and rapid detection of foodborne pathogens. Biotechnol. Adv. 36 (4), 1003–1024. https://doi.org/10.1016/j.biotechadv.2018.03.002.
Kim, M., Jung, T., Kim, Y., Lee, C., Woo, K., Seol, J.H., Yang, S., 2015. A microfluidic device for label-free detection of Escherichia coli in drinking water using positive dielectrophoretic focusing, capturing, and impedance measurement. Biosens. Bioelectron. 74, 1011–1015. https://doi.org/10.1016/j.bios.2015.07.059.
Lawton, J.W., 2002. Zein: a history of processing and use. Cereal Chem. 79 (1), 1–18. https://doi.org/10.1094/CCHEM.2002.79.1.1.
Li, H., Wang, D., Liu, C., Zhu, J., Fan, M., Sun, X., et al., 2019. Fabrication of stable zein nanoparticles coated with soluble soybean polysaccharide for encapsulation of quercetin. Food Hydrocolloids 87 (August 2018), 342–351. https://doi.org/10.1016/j.foodhyd.2018.08.002.
Lin, Q., Liang, R., Zhong, F., Ye, A., Singh, H., 2018. Physical properties and biological fate of OSA-modified-starch-stabilized emulsions containing β-carotene: effect of calcium and pH. Food Hydrocolloids 77, 549–556. https://doi.org/10.1016/j.foodhyd.2017.10.033.
Mark, D., Haeberle, S., Roth, G., von Stetten, F., Zengerle, R., 2010. Microfluidic lab-on-a-chip platforms: requirements, characteristics and applications. Chem. Soc. Rev. 39 (3), 1153. https://doi.org/10.1039/b820557b.
Martínez-Ramos, A.R., Ibarra-Sánchez, L.A., Amaya-Llano, S.L., Miller, M.J., 2020. Evaluation of combinations of nisin, lauric arginate, and ε-polylysine to control Listeria monocytogenes in queso fresco. J. Dairy Sci. 103 (12), 11152–11162. https://doi.org/10.3168/jds.2020-19001.
Marze, S., Algaba, H., Marquis, M., 2014. A microfluidic device to study the digestion of trapped lipid droplets. Food Funct. 5 (7), 1481–1488. https://doi.org/10.1039/c4fo00010b.
Micsonai, A., Wien, F., Kernya, L., Lee, Y.H., Goto, Y., Réfrégiers, M., Kardos, J., 2015. Accurate secondary structure prediction and fold recognition for circular dichroism spectroscopy. Proc. Natl. Acad. Sci. U.S.A. 112 (24), E3095–E3103. https://doi.org/10.1073/pnas.1500851112.
Nguyen, H.T., Marquis, M., Anton, M., Marze, S., 2019a. Studying the real-time interplay between triglyceride digestion and lipophilic micronutrient bioaccessibility using droplet microfluidics. 2 application to various oils and (pro)vitamins. Food Chem. 275 (July 2018), 661–667. https://doi.org/10.1016/j.foodchem.2018.09.126.
Nguyen, H.T., Marquis, M., Anton, M., Marze, S., 2019b. Studying the real-time interplay between triglyceride digestion and lipophilic micronutrient bioaccessibility using droplet microfluidics. 2 application to various oils and (pro)vitamins. Food Chem. 275 (July 2018), 661–667. https://doi.org/10.1016/j.foodchem.2018.09.126.
Özel, B., Şimşek, Ö., Akçelik, M., Saris, P.E.J., 2018. Innovative approaches to nisin production. Appl. Microbiol. Biotechnol. 102 (15), 6299–6307. https://doi.org/10.1007/s00253-018-9098-y.
Patel, A.R., Velikov, K.P., 2014. Zein as a source of functional colloidal nano- and microstructures. Curr. Opin. Colloid Interface Sci. 19 (5), 450–458. https://doi.org/10.1016/j.cocis.2014.08.001.
Priest, C., Reid, M.D., Whitby, C.P., 2011. Formation and stability of nanoparticle-stabilised oil-in-water emulsions in a microfluidic chip. J. Colloid Interface Sci. 363 (1), 301–306. https://doi.org/10.1016/j.jcis.2011.07.060.
Ravanfar, R., Comunian, T.A., Dando, R., Abbaspourrad, A., 2018. Optimization of microcapsules shell structure to preserve labile compounds: a comparison between microfluidics and conventional homogenization method. Food Chem. 241 (June 2017), 460–467. https://doi.org/10.1016/j.foodchem.2017.09.023.
Shin, J.M., Gwak, J.W., Kamarajan, P., Fenno, J.C., Rickard, A.H., Kapila, Y.L., 2016. Biomedical applications of nisin. J. Appl. Microbiol. 120 (6), 1449–1465. https://doi.org/10.1111/jam.13033.
Sweedman, M.C., Tizzotti, M.J., Schäfer, C., Gilbert, R.G., 2013. Structure and physicochemical properties of octenyl succinic anhydride modified starches: a review. Carbohydr. Polym. 92 (1), 905–920. https://doi.org/10.1016/j.carbpol.2012.09.040.
Teh, S.Y., Lin, R., Hung, L.H., Lee, A.P., 2008. Droplet microfluidics. Lab Chip 8 (2), 198–220. https://doi.org/10.1039/b715524g.
Van Tassell, M.L., Ibarra-Sánchez, L.A., Takhar, S.R., Amaya-Llano, S.L., Miller, M.J., 2015. Use of a miniature laboratory fresh cheese model for investigating antimicrobial activities. J. Dairy Sci. 98 (12), 8515–8524. https://doi.org/10.3168/jds.2015-9967.
Zhang, B., Luo, Y., Wang, Q., 2011. Effect of acid and base treatments on structural, rheological, and antioxidant properties of α-zein. Food Chem. 124 (1), 210–220. https://doi.org/10.1016/j.foodchem.2010.06.019.
Zhao-Miao, L.I.U., Yu, D.U., Yan, P.A.N.G., 2018. Generation of water-in-oil-in-water (W/O/W) double emulsions by microfluidics. Chin. J. Anal. Chem. 46 (3), 324–330. https://doi.org/10.1016/S1872-2040(17)61072-7.